JOURNAL OF THERMOPHYSICS AND HEAT TRANSFER
Vol. 21, No. 1, January–March 2007

Void Fraction Measurement of Gas–Liquid Two-Phase Flow Using Magnetic Fluid

Takuya Kuwahara* and Hiroshi Yamaguchi†
Doshisha University, Kyoto 610-0321, Japan

DOI: 10.2514/1.17650

This paper describes a new measuring technique of void fraction using magnetic fluid. The proposed measurement can be realized with simple devices. The present study consists of two appropriate experiments termed "static experiment" ("calibration test") and "flow experiment" ("actual flow test"). In the present study, the experiments have been performed with fully diluted magnetic fluid for the purpose of applying to common two-phase flow situations such as air–water. Results of the experiments have concluded that the proposed measuring technique of void fraction can measure void fraction in air–water two-phase flow situations by adding a small amount of magnetic fluid to fluids of interest. The present method has promise for other fluids.

Nomenclature

A	=	area of cross section of pipe, m^2
$\boldsymbol{B}$	=	magnetic flux density, T for tesla
$\boldsymbol{H}$	=	magnetic field, A/m for ampere/m
H	=	magnitude of magnetic field, A/m
j	=	volumetric flux, m/s
k	=	Boltzmann constant, J/K
$\boldsymbol{M}$	=	magnetization, A/m
m	=	magnetic moment of a magnetic particle, $A \cdot m^2$
N	=	demagnetizing factor
n	=	number of windings of induction coil
n_0	=	number of particles per unit volume, m^{-3}
P	=	pressure, Pa
Q	=	flow rate, m^3/s
S	=	inner area of induction coil, m^2
T	=	absolute temperature, K
V	=	induced electromotive force, V for voltage
X, Y, Z	=	Cartesian coordinates (see Figs. 6 and 7)
α	=	void fraction
$\Delta\boldsymbol{B}$	=	differential magnetic flux density, T
ΔV	=	differential voltage, V
ε	=	induced electromotive force in a circle, V
μ	=	permeability
μ_0	=	vacuum permeability
χ_m	=	magnetic susceptibility

Subscripts

d	=	demagnetization
g	=	gaseous phase
l	=	liquid phase
mf	=	magnetic fluid or diluted magnetic fluid
mix	=	two-phase state
rms	=	root mean square value (effective value)
void	=	air bubble in diluted magnetic fluid
1	=	before closing valves
2	=	after closing valves

Received 21 May 2005; revision received 19 August 2006; accepted for publication 26 August 2006.

*Ph.D. Student, Department of Mechanical Engineering; ete1301@-mail4.doshisha.ac.jp.

†Professor, Department of Mechanical Engineering; hyamaguc@mail.-doshisha.ac.jp.

I. Introduction

GAS–LIQUID two-phase flow can be seen in various applications such as boiling water reactors (BWR), industrial boilers, chemical processing plants, petroleum engineering using gas-lift pumps, and medical applications using microbubbles. There are strong reasons why two-phase flow should be studied and analyzed because gas–liquid two-phase flow plays important roles in industrial applications. However, knowledge of two-phase flow and measuring techniques as related to key parameters are not sufficient so far because the phenomena in two-phase flow are quite complex. There are many parameters in two-phase flow. Among them, the void fraction, which is the ratio of the gaseous phase volume to the total control volume, is particularly significant.

Existing measuring methods for void fraction include the differential pressure method, the quick-closing valves method [1], the needle contact probe method [2], the optical fiber probe method [3], the conductance method [4,5], the capacitance method [6], the x-ray scanning method [7], and neutron radiography [8]. In recent years, measurement using wire-mesh tomography has been studied [9,10]. Among these techniques, the quick-closing valves method and the needle contact probe method are widely used because these techniques enable us to obtain the void fraction easily without extensive instrumentation. However, these measuring methods have some problems. For example, the quick-closing valves method requires stopping the flow, and the measured value of void fraction often includes large errors in the high void fraction region. The needle contact probe method needs a sufficiently thin needle (several μm) as a sensing element. The procedure for making very thin needles is not easy.

As mentioned above, establishment of a new simple measuring method for void fraction has important consequences. The present study proposes a new measurement technique using a fully diluted magnetic fluid. The magnetic fluid is a magnetizable liquid which has many applications [11]. The measuring method is based on the idea that there is a relationship between the space distribution of air bubbles and the distribution of the magnetization within a diluted magnetic fluid. The proposed measuring technique does not require any pipe processes and can be realized as an easy measurement of void fraction because the measurement is carried out by using electromagnetic induction. The measuring technique is also available for applications using gas–liquid two-phase flow in pure and mixtures of magnetic fluids [12,13]. The purpose of this study is to establish the proposed measuring technique of the void fraction.

II. Experiment

A. Principle of Measurement

In the case that directions of the magnetic field and magnetization are parallel, the magnetic flux density $\boldsymbol{B}$ is given by the following

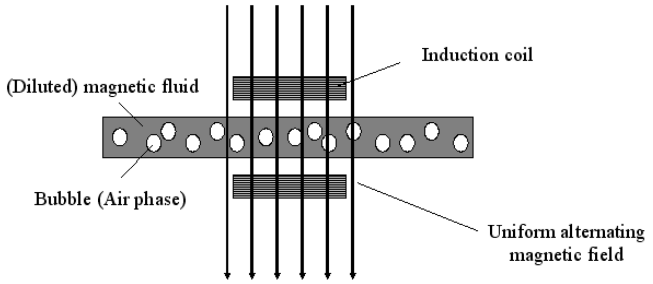

Fig. 1 Process schematic for the present measurement of the void fraction.

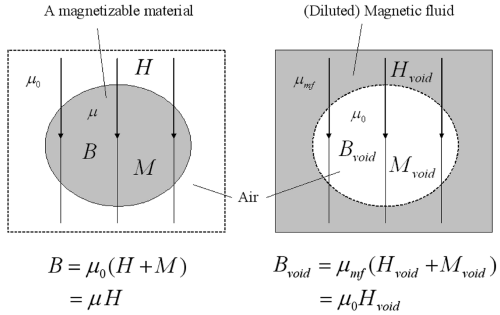

Fig. 2 Magnetic flux density through a two-phase state.

formula [14]:

$$\boldsymbol{B} = \mu_0(\boldsymbol{H} + \boldsymbol{M}) \tag{1}$$

where μ_0 is the vacuum permeability. Furthermore, Eq. (1) can also be expressed by the following formula with the permeability μ:

$$\boldsymbol{B} = \mu \boldsymbol{H} \tag{2}$$

As shown in Fig. 1, when a pipe containing a magnetic fluid is set in the middle of a uniform magnetic field, the magnetic flux density $\boldsymbol{B}_{\text{mix}}$ passed through the magnetic fluid which includes bubbles can be written by the following formula:

$$\boldsymbol{B}_{\text{mix}} = \mu_0(\boldsymbol{H} + \boldsymbol{M}_{\text{mix}}) \tag{3}$$

where $\boldsymbol{M}_{\text{mix}}$ is the magnetization of magnetic fluid including a gaseous phase (bubbles) and is a function of α (the ratio of gas phase volume to the whole volume). This formula is based on the assumption that, in the case that the resultant magnetic field $\boldsymbol{H}$ is constant, the magnetization of the magnetic fluid depends on the void fraction. It is noted that the magnetic susceptibility of the gaseous phase (in this case, air) is on the order of 10^{-7} and can be neglected. In the case of an induction coil whose number of windings is one, the induced electromotive force can be written as follows by using Faraday's law [15]:

$$\varepsilon = -\frac{\partial}{\partial t}\iint_S \boldsymbol{B}\cdot\hat{\boldsymbol{n}}\,\mathrm{d}S \tag{4}$$

Considering Eq. (3), the induced electromotive force generated in a set of induction coils with n windings is written as follows:

$$V = -n\frac{\partial}{\partial t}\iint_S [\mu_0\{\boldsymbol{H} + \boldsymbol{M}_{\text{mix}}\}\cdot\hat{\boldsymbol{n}}]\,\mathrm{d}S \tag{5}$$

Specifically, the induced electromotive force in the induction coils is uniquely determined by void fraction when $\boldsymbol{H}$ is given and known. In other words, void fraction can be measured by measuring the induced electromotive force in the induction coils.

B. Magnetization of Magnetic Fluid Including Gaseous Phase

The magnetization of a magnetic fluid which includes the gaseous phase is discussed here. The following two models are proposed in the present study. One is a model considering the shape of the gaseous phase (bubbles). Another is a simple model which does not consider the shape of the gaseous phase.

C. Model that Considers Shape of Gaseous Phase (Bubbles)

When a bubble exists in a magnetic fluid, magnetic polarization occurs at the interface between the gaseous phase and the magnetic fluid. Thus, the bubble behaves like a magnetized substance. The bubble has demagnetization whose direction is opposite to that of the magnetization of the magnetic fluid. The magnitude of magnetization in the bubble can be expressed by using a demagnetizing factor because the magnitude depends on the shape of the bubble.

In the case that a bubble exists in a magnetic fluid, the magnetization caused by the bubble can be expressed as follows:

$$\boldsymbol{B}_{\text{void}} = \mu_{\text{mf}}(\boldsymbol{H}_{\text{void}} + \boldsymbol{M}_{\text{void}}) \tag{6}$$

where μ_{mf} is the permeability of the magnetic fluid, $\boldsymbol{H}_{\text{void}}$ is the magnetic field of the bubble, and $\boldsymbol{M}_{\text{void}}$ is the magnetization of the bubble. To obtain Eq. (6), Fig. 2 shows a schematic of correspondence between Eqs. (1) and (6). In the same manner as Eq. (2), Eq. (6) can also be expressed by

$$\boldsymbol{B}_{\text{void}} = \mu_0 \boldsymbol{H}_{\text{void}} \tag{7}$$

From Eq. (6), the magnetization of the bubble is written by the following formula:

$$\boldsymbol{M}_{\text{void}} = \frac{\boldsymbol{B}_{\text{void}}}{\mu_{\text{mf}}} - \boldsymbol{H}_{\text{void}} = \left(\frac{\mu_0}{\mu_{\text{mf}}} - 1\right)\boldsymbol{H}_{\text{void}} \tag{8}$$

The magnetic field $\boldsymbol{H}_{\text{void}}$ of the bubble is expressed with the superposition of the outer magnetic field $\boldsymbol{H}$ and the demagnetization caused by the magnetic polarization:

$$\boldsymbol{H}_{\text{void}} = \boldsymbol{H} - \boldsymbol{H}_d \tag{9}$$

In view of the following formula on the demagnetization [16]:

$$\boldsymbol{H}_d = N\boldsymbol{M}_{\text{void}} \tag{10}$$

where N depends on the shape of the bubble. The magnetic field of the bubble $\boldsymbol{H}_{\text{void}}$ can be derived as follows:

$$\boldsymbol{H}_{\text{void}} = \boldsymbol{H} - \boldsymbol{H}_d = \boldsymbol{H} - N\boldsymbol{M}_{\text{void}} \tag{11}$$

From Eqs. (8) and (11), the magnetic field of the bubble $\boldsymbol{H}_{\text{void}}$ can be rewritten as follows:

$$\boldsymbol{H}_{\text{void}} = \frac{\mu_{\text{mf}}}{(1-N)\mu_{\text{mf}} + N\mu_0}\boldsymbol{H} \tag{12}$$

From Eqs. (8) and (12), a bubble in a magnetic fluid has magnetization given by the following formula:

$$\boldsymbol{M}_{\text{void}} = -\frac{\mu_{\text{mf}} - \mu_0}{(1-N)\mu_{\text{mf}} + N\mu_0}\boldsymbol{H} \tag{13}$$

Based on the definition of the magnetization, a product of the magnetization and the volume ratio of the magnetization can be used as the total magnetization in a control volume [12]. Hence, the magnetic flux density $\boldsymbol{B}_{\text{mix}}$ passed through the magnetic fluid which includes bubbles can also be expressed as follows by employing α:

$$\boldsymbol{B}_{\text{mix}} = \mu_{\text{mf}}(\boldsymbol{H} + \alpha\boldsymbol{M}_{\text{void}}) \tag{14}$$

In the same manner as Eq. (2), $\boldsymbol{B}_{\text{mix}}$ can also be obtained with a total magnetic permeability of the magnetic fluid which includes bubbles:

$$\boldsymbol{B}_{\text{mix}} = \mu_{\text{mix}}\boldsymbol{H} \tag{15}$$

From Eqs. (13–15), the following formula is obtained:

$$\mu_{\mathrm{mix}}\boldsymbol{H} = \mu_{\mathrm{mf}}\boldsymbol{H} - \alpha\frac{\mu_{\mathrm{mf}}(\mu_{\mathrm{mf}}-\mu_0)}{(1-N)\mu_{\mathrm{mf}}+N\mu_0}\boldsymbol{H} \tag{16}$$

Therefore, when bubbles exist in a magnetic fluid, the total magnetic permeability of the magnetic fluid can be expressed by the following formula:

$$\mu_{\mathrm{mix}} = \mu_{\mathrm{mf}} - \alpha\frac{\mu_{\mathrm{mf}}(\mu_{\mathrm{mf}}-\mu_0)}{(1-N)\mu_{\mathrm{mf}}+N\mu_0} \tag{17}$$

In particular, for spherical bubbles ($N = 1/3$), the total magnetic permeability of the magnetic fluid can be expressed by the following formula [17,18]:

$$\mu_{\mathrm{mix}} = \mu_{\mathrm{mf}} - \alpha\frac{3\mu_{\mathrm{mf}}(\mu_{\mathrm{mf}}-\mu_0)}{2\mu_{\mathrm{mf}}+\mu_0} \tag{18}$$

In view of Eq. (1), the magnetic flux density in a magnetic fluid can be described by

$$\boldsymbol{B}_{\mathrm{mf}} = \mu_0(\boldsymbol{H}+\boldsymbol{M}_{\mathrm{mf}}) \tag{19}$$

Then, the following formula can be obtained by introducing the magnetic susceptibility χ_m of the magnetic fluid:

$$\boldsymbol{B}_{\mathrm{mf}} = \mu_0(\boldsymbol{H}+\chi_m\boldsymbol{H}) = \mu_0(1+\chi_m)\boldsymbol{H} \tag{20}$$

Taking account of Eq. (2), the magnetic flux density in a magnetic fluid can also be described as follows:

$$\boldsymbol{B}_{\mathrm{mf}} = \mu_{\mathrm{mf}}\boldsymbol{H} \tag{21}$$

From Eqs. (20) and (21), the permeability μ_{mf} of the magnetic fluid can be written as follows [16,19]:

$$\mu_{\mathrm{mf}} = \mu_0(1+\chi_m) \tag{22}$$

In the system under consideration, however, when there is a magnetic fluid in a container or a pipe such as our measurement, total magnetization in a control volume decreases when void fraction increases. This effect affects the demagnetization in the bubbles. In view of this effect, total permeability in pipe flow can be assumed to be a function of the void fraction as follows:

$$\mu_{\mathrm{mf}} = \mu_0\{1+(1-\alpha)\chi_m\} \tag{23}$$

It is noted that this expression can be valid only for the permeability μ_{mf} which affects the demagnetization in Eq. (13) so that Eq. (13) is rewritten by using Eq. (23) as follows:

$$\boldsymbol{M}_{\mathrm{void}} = -\frac{(1-\alpha)\chi_m}{(1-N)\{1+(1-\alpha)\chi_m\}+N}\boldsymbol{H} \tag{24}$$

In the system under consideration, Eq. (11) is thus rewritten by the following formula:

$$\boldsymbol{H}_{\mathrm{void}} = \boldsymbol{H} - \alpha\boldsymbol{H}_d = \boldsymbol{H} - \alpha N\boldsymbol{M}_{\mathrm{void}} \tag{25}$$

because the demagnetization in the control volume depends on the void fraction. The magnetization of the magnetic fluid which includes a gaseous phase is given by the following formula:

$$\boldsymbol{M}_{\mathrm{mix}} = (1-\alpha)\chi_m\boldsymbol{H}_{\mathrm{void}} \tag{26}$$

Using Eqs. (24) and (25), Eq. (26) can be expressed as follows:

$$\begin{aligned}\boldsymbol{M}_{\mathrm{mix}} &= (1-\alpha)\left(1+\alpha\frac{N(1-\alpha)\chi_m}{(1-N)\{1+(1-\alpha)\chi_m\}+N}\right)\chi_m\boldsymbol{H}\\ &= (1-\alpha)\left(1+\alpha\frac{N(1-\alpha)\chi_m}{(1-N)\{1+(1-\alpha)\chi_m\}+N}\right)\boldsymbol{M}_{\mathrm{mf}}\end{aligned} \tag{27}$$

The magnetic flux density $\boldsymbol{B}_{\mathrm{mix}}$ can be expressed by the following formula:

$$\begin{aligned}\boldsymbol{B}_{\mathrm{mix}} = \mu_0\{\boldsymbol{H}+\boldsymbol{M}_{\mathrm{mix}}\} = \mu_0\{\boldsymbol{H}+(1-\alpha)\chi_m\boldsymbol{H}_{\mathrm{void}}\} = \mu_0\Bigg[\boldsymbol{H}\\ +(1-\alpha)\left(1+\alpha\frac{N(1-\alpha)\chi_m}{(1-N)\{1+(1-\alpha)\chi_m\}+N}\right)\boldsymbol{M}_{\mathrm{mf}}\Bigg]\end{aligned} \tag{28}$$

It is noted that a fluid mixture which includes magnetic fluid in the relative amount of 0.1% by volume was used as a working fluid in the present study. This fluid mixture of distilled water and magnetic fluid is termed "diluted magnetic fluid of 0.1% by volume." In the weak magnetic field of the present study, the magnetic susceptibility χ_m, of a diluted magnetic fluid which is 0.1% by volume is approximately 0.20×10^{-3}, which is obtained from parameters of the water-based magnetic fluid [20]. In general, the magnetization of a magnetic fluid can be expressed by using the following Langevin function [21]:

$$\begin{aligned}&M_{\mathrm{mf}} = n_0 mL\left(\frac{\mu_0 mH}{kT}\right)\\ &[L(\xi) = \coth(\xi) - \xi^{-1}\text{: Langevin function}]\end{aligned} \tag{29}$$

From Eqs. (28) and (29), the assumption that the magnetization of a magnetic fluid depends on the void fraction is appropriate when the magnetic field $\boldsymbol{H}$ and temperature T are constants.

D. Model Not Considering Shape of the Gaseous Phases

Based on the simple assumption that a spatial distribution of air bubbles and a distribution of magnetization within a magnetic fluid are equivalent, the magnetization of a magnetic fluid which includes a gaseous phase is expressed by the following formula:

$$\boldsymbol{M}_{\mathrm{mix}} = (1-\alpha)\boldsymbol{M}_{\mathrm{mf}} \tag{30}$$

In this case, Eq. (3) is rewritten as follows:

$$\boldsymbol{B}_{\mathrm{mix}} = \mu_0\{\boldsymbol{H}+(1-\alpha)\boldsymbol{M}_{\mathrm{mf}}\} \tag{31}$$

In Eq. (31), there is a linear relationship between void fraction and magnetic flux density passed through the magnetic fluid.

E. Comparison of the Two Models

The differential magnetic flux density that is the magnetic flux density induced in a magnetic fluid can be defined as follows:

$$\Delta\boldsymbol{B} = \boldsymbol{B}_{\mathrm{mix}(\alpha=\alpha)} - \boldsymbol{B}_{\mathrm{mix}(\alpha=1)} \tag{32}$$

The differential magnetic flux densities in the two models are obtained from Eq. (28) and from Eq. (31) as follows:

$$\Delta\boldsymbol{B} = \mu_0(1-\alpha)\left[1+\alpha\frac{N(1-\alpha)\chi_m}{(1-N)\{1+(1-\alpha)\chi_m\}+N}\right]\boldsymbol{M}_{\mathrm{mf}} \tag{33}$$

$$\Delta\boldsymbol{B} = \mu_0(1-\alpha)\boldsymbol{M}_{\mathrm{mf}} \tag{34}$$

Figure 3 shows the results of the comparison between Eqs. (33) and (34). In the comparison, the demagnetizing factor is given as 0.333 [16] in the bubbly flow regime (void fraction 0–0.3), and it is given as 0.50 [16] in the slug flow and the annular flow regimes (void fraction 0.3–1.0). In the case of a diluted magnetic fluid of 0.1% by volume, Fig. 3 shows that the maximum difference was less than 0.0015% in all flow regimes. The proposed measuring technique results from using a simple model that does not consider the bubble shape and yields an error of 0.0015%. Taking into account the results, the linear relationship between void fraction and magnetic flux density passed through a magnetic fluid was considered to be accurate.

F. Test Fluid

Water-based magnetic fluid (Taiho Industries Co., Ltd: W-40) was used as a model working fluid. The water-based magnetic fluid is

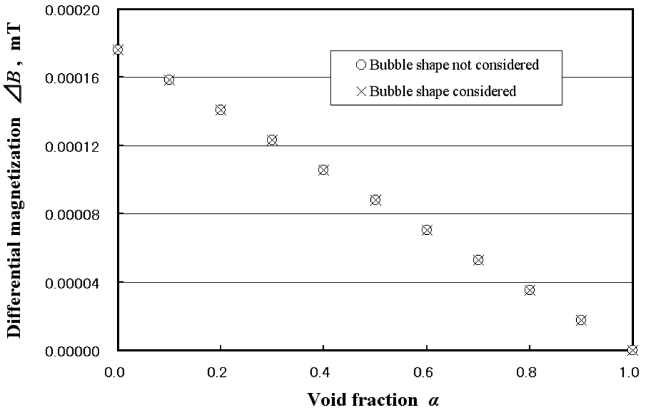

Fig. 3 Difference of magnetic flux density caused by a bubble shape.

dissolvable in water. Table 1 shows the basic properties of the magnetic fluid used in the present study. It is noted that the magnetization of this magnetic fluid has low dependence on temperature.

G. Experimental Setup

Figure 4 schematically shows the stationary state experimental apparatus. Figure 5 shows the experimental apparatus for flowing conditions. The experiment under stationary conditions is termed the "static experiment," and the experiment under flowing conditions is termed the "flow experiment." In the flow experiment, flow is generated by a pump. The main components of the equipment in Figs. 4 and 5 are explained below:

1. Excitation Coil (Helmholtz Coil)

Two Helmholtz coils were used as excitation coils. The Helmholtz coil was designed to generate a large uniform magnetic field. As shown in Figs. 4 and 5, one of the two Helmholtz coils was used in the main measuring section. Another one was used in the reduction section of the experimental setup. The same arrangement of excitation coils was used in the static and flow experiments. Figure 6 shows the arrangement of the coils in detail. The characteristics of the excitation coils are shown in Fig. 7. In the present study, the pair of coils could generate a uniform magnetic field as shown in Fig. 8. A representative example of the electric current in the excitation coil is 0.25 A. Acrylic resin was used as a mounting material to prevent eddy currents, which might deform the uniform magnetic field. The magnetic flux density at the center of the uniform magnetic field was 0.33 mT.

2. Induction Coil (Secondary Coil)

The induction coil plays the role of detecting electromotive force which is a function of void fraction. The same induction coils were used in both the static and flow experiments. Figure 6 also describes the arrangement of the induction coils. The characteristics of the rectangular induction coil are shown in Fig. 7.

3. Reduction Coil

The reduction coil, which has the same characteristics as the induction coil, was used to increase detection rates of induced electromotive force caused by magnetization of the magnetic fluid.

Table 1 Properties of pure magnetic fluid, diluted magnetic fluid of 0.1% by volume, and distilled water

	Magnetic fluid, 296 K	Diluted magnetic fluid	Distilled water
Density, 10^3 kg/m^3	1.410	1.00	1.00
Viscosity, mPa · s	18.85	1.011	1.008
Surface tension, mN/m	38.90	70.4	72.1

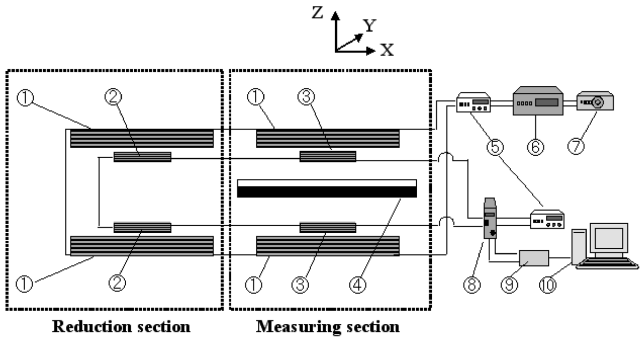

Fig. 4 Schematic diagram of static experimental apparatus.

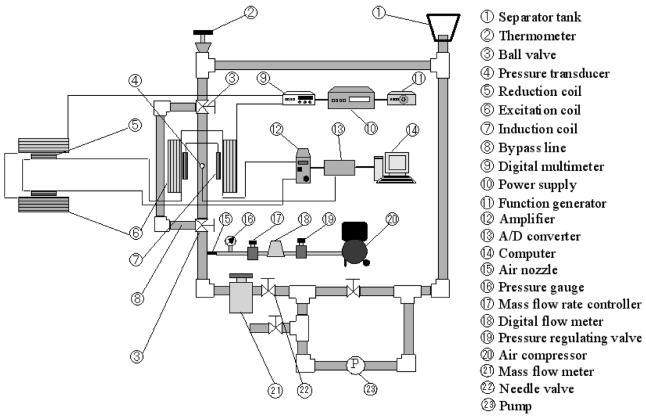

Fig. 5 Schematic diagram of flow experimental apparatus.

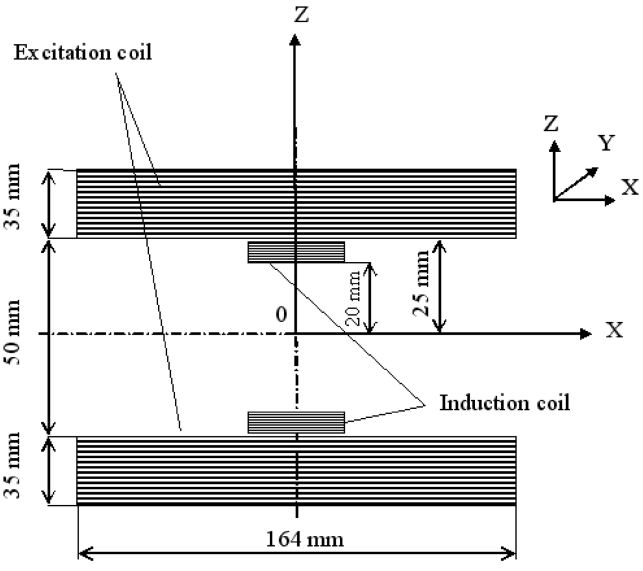

Fig. 6 Arrangement of coils.

This coil was connected in a series with the induction coil to cancel the excess electromotive force generated by the induction coils. It is noted that the excess electromotive force is detected as base voltage not caused by the magnetization of the magnetic fluid or the diluted magnetic fluid, but merely due to inductance of the coil itself. In the experiments, the rectangular reduction coils were placed inside of the

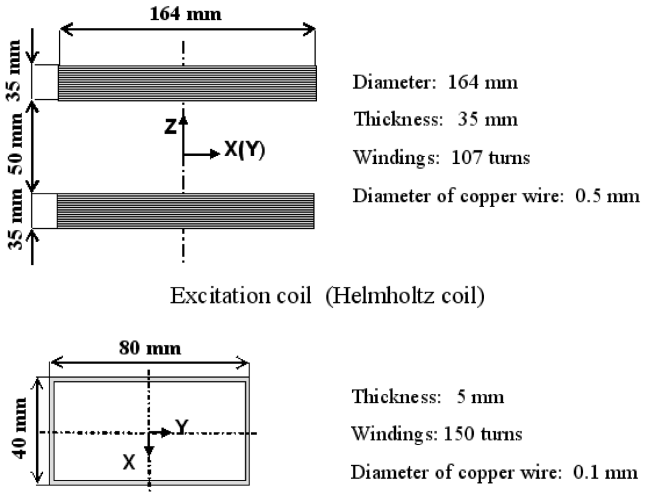

Fig. 7 Details of excitation coils and induction coils.

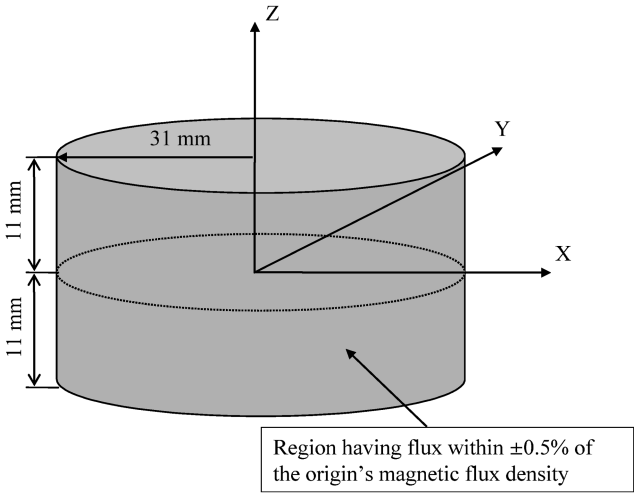

Fig. 8 Region of uniform magnetic field.

excitation coil in the reduction section in order to have the same coil arrangement as in the measuring section of the apparatus.

4. Magnetic Fluid Test Plug

Magnetic fluid test plugs were used in the static experiment and play the role of giving calibration data for actual pipe flow measurements as functions of the void fraction and the electromotive force, that is, the flow experiment. Each magnetic fluid plug contains a measured amount of a diluted magnetic fluid to obtain void fraction from 0–1.0 (interval is 0.1) as shown in Fig. 9. These containers were made of acrylic resin whose magnetization is negligible. An acrylic resin pipe, whose inner diameter was 12 mm, was the same size as the pipe used in the flow experiment. The length of the magnetic test plug was 300 mm.

5. Data Acquisition System

The instantaneous induced electromotive force was converted to digital signals by an analog-digital converter (A/D converter) installed in a PC because the induced electromotive force caused by the bubbles was not stable in the flow experiment. Sampling frequency was 10,000 Hz and the total number of samples was 30,000, that is, the sampling time (measuring time) was 3 s. Data such as pressure and flow rates of the gaseous and liquid phases were also converted into digital data. The characteristics of the A/D converter

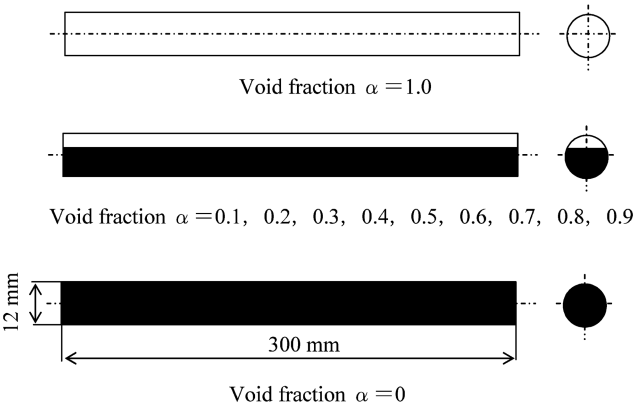

Fig. 9 Magnetic fluid test plugs.

were ±10 V input voltage and 16 bit resolution. Time response in the data acquisition system was 10^{-5} s. It is also noted that the time response caused by the properties of the magnetic fluid was approximately 10^{-6} s, which is the Brownian relaxation time.

6. Air Injection

As shown in Fig. 5, an air injection section was installed. Air injectors were included in the system with an air compressor, an oil filter, a pressure regulating valve, a digital flow meter, a flow controller, and a pressure gauge. The pressure regulating valve supplied stable air to the flow controller. Two small copper pipes whose diameters were 0.1 mm were used as bubble injectors. The two injectors were kept 25 mm apart so that the bubbles injected into the main flow passage did not interfere with each other.

H. Experimental Method

In this study, the static experiment was first performed to obtain a relationship between the induced electromotive force (differential voltage mentioned below) and the void fraction. From this relationship, a calibration curve was found in each experiment. Next, the flow experiment was performed to obtain data in an actual vertical gas–liquid two-phase flow. A relationship between the void fraction and the electromotive force was found from the static experiment. The obtained relationship was used as a calibration curve in the flow experiment. The relationship between the void fraction and the electromotive force obtained from the flow experiment was compared with the calibration curve to verify the validity of the proposed measurement method. Details of the static experiment and the flow experiment are explained below.

1. Static Experiment

As shown in Fig. 4, the induced electromotive forces were measured by installing the magnetic fluid test plugs in the middle of a uniform magnetic field. A digital multimeter was used as a monitor because it was impossible to calculate the root mean square value of voltage in real time by using the obtained digital data. Then the detected electromotive forces were converted into digital data. Noise included in these data was removed by a filter. Finally, the root mean square value of voltage was calculated. In this study, the differential value between electromotive force at a void fraction of 1.0 (no magnetic fluid) and electromotive force at chosen void fractions was termed "differential voltage," and the differential voltage was used as the main parameter which is equivalent to the induced voltage caused by only magnetization of the magnetic fluid.

$$\Delta V = V_{\mathrm{rms}(\alpha=\alpha)} - V_{\mathrm{rms}(\alpha=1.0)} \tag{35}$$

where V_{rms} indicates the root mean square value of voltage.

The static experiment for creating the calibration curves between the void fraction and the differential voltage was performed under the same conditions on the electric current of the excitation coils and the temperature as the corresponding flow experiment.

2. Flow Experiment

The apparatus of the flow experiment could produce an actual vertical upward moving gas–liquid two-phase flow of a diluted magnetic fluid. In the experimental setup shown in Fig. 5, a magnetic fluid flows in the clockwise direction. The test section (measuring section) was the vertical pipe situated between the two ball valves in Fig. 5. The air injectors were positioned at the lower part of the test section. The bubbles (gaseous phase) in two-phase flow were removed in the separator tank, which was installed as shown in Fig. 5. The diluted magnetic fluid remained as only the liquid phase at the separator tank and was recirculated. The flow experiment was conducted by regulating volumetric flux of the gaseous phase and volumetric flux of the liquid phase. The volumetric flux is one of the significant parameters in two-phase flow. The volumetric flux of the gaseous phase j_g and the volumetric flux of the liquid phase j_l are defined as follows:

$$j_g = \frac{Q_g}{A} \tag{36}$$

$$j_l = \frac{Q_l}{A} \tag{37}$$

where Q_g is the flow rate of the gaseous phase, Q_l is the flow rate of the liquid phase, and A is the cross-sectional area of flow. The inner diameter of the cylindrical pipe was 12 mm. This pipe was made from clear acrylic resin to allow reading height of the magnetic fluid when measuring void fraction by the quick-closing valves method. Figure 9 shows the principle of the quick-closing valves method. The void fraction could be calculated from the height of the liquid phase (magnetic fluid) after closing the valves.

In this experiment, 3-direction ball valves equipped with air actuators (see Fig. 5) were located at the inlet and outlet of the test section. These valves could be closed suddenly at the same time by the actuator. When the valves closed, the flow was routed through the bypass line. The length of the test section was 540 mm. A pressure port was connected to the pressure transducer and was located in the middle of the test section. In the flow experiment, differential voltage was first measured, and void fraction was found by the quick-closing valves method (see Fig. 10) at the same section as the voltage measurement. The amplified electromotive force was converted into digital data. The digital voltage data were processed as the root mean square value in the same manner as done for the static experiment, to obtain the differential voltage.

In addition, the pressure in the test section was measured since the pressure was changed when the ball valves were closed for measurement of void fraction by the quick-closing valves method. This change of pressure could affect or change the void fraction. Hence, the measured void fraction was corrected by the following formula derived from Boyle's law [22]:

$$\alpha_1 = \frac{P_2}{P_1}\alpha_2 \tag{38}$$

where α_1 is the void fraction before closing the valves, α_2 is the void fraction after closing the valves, P_1 is the absolute pressure before closing valves, and P_2 is the absolute pressure after closing valves.

III. Results and Discussion

A. Physical Properties of Diluted Magnetic Fluid

Before running the experiments, physical properties (viscosity, density, and surface tension) of the diluted magnetic fluid of 0.1% by volume were measured without a magnetic field at a room temperature of 23°C (296 K), which is the same temperature as used for the experiments. The measurements were carried out using an Ostwald viscometer, Baume hydrometers, and a DuNouy tensiometer, respectively.

Table 1 shows the measured properties of the magnetic fluid, diluted magnetic fluid of 0.1% by volume, and distilled water. These results suggest that the physical properties of viscosity and density

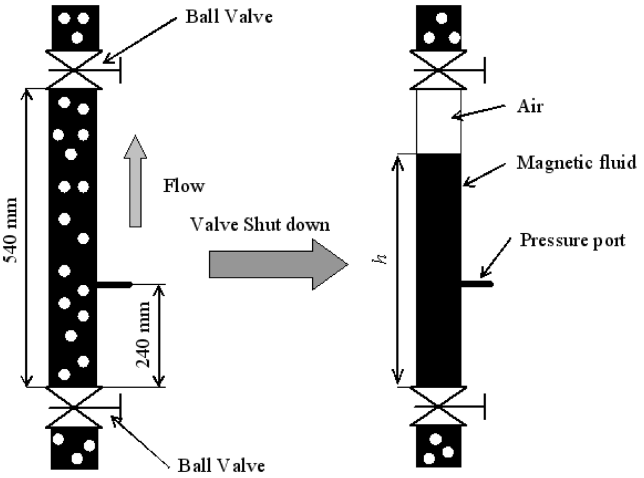

Fig. 10 Principle of operation for quick-closing valves method.

were almost the same values as the physical properties of distilled water. That is, the kinetic viscosity was almost the same value for the diluted magnetic fluid and the distilled water. The surface tension of the magnetic fluid σ was 70.4 mN/m which is close to the surface tension of distilled water, 72.1 mN/m. This is because the kinematic viscosity and the surface tension, which influence the characteristics of two-phase flow, were almost the same for the diluted magnetic fluid and the distilled water. It is further noted that the simple addition of magnetic fluid to water at a concentration of 0.1% by volume for measuring the void fraction would yield the same flow as air–water two-phase flow.

B. Static Experiment

To obtain the calibration curve for the flow experiment, the static experiments were performed under the conditions that the input electric current was 0.25 A, the frequency of the input electric current was 1000 Hz, and the amplifier gain was 500. As estimated by the theoretical approach, good linearity between the differential voltage and the void fraction was obtained as shown in Fig. 11. Thus, the calibration curve for the flow experiment was taken to be approximately linear. The mean absolute error of data from the calibration curve was 2.3% (0.023 by void fraction). The maximum absolute error of data from the calibration curve was 5.1% (0.051 by void fraction) at a void fraction of 0 in Fig. 11. The other data errors were less than 3.0%. The calibration curve (line) is shown with the results of the flow experiments as seen in the following section.

C. Flow Experiment

Before the flow experiments of void fraction measurement, a verification experiment was carried out to investigate the differences in the flow regimes for diluted magnetic fluid of 0.1% by volume as compared to distilled water under the same conditions on the volumetric flux of each phase. For this comparison, the volumetric flux values of the liquid phase were 0 and 0.042 m/s, and the volumetric flux values of the gaseous phase were 0–0.206 m/s. Visualization was performed by regulating the volumetric flux of the gaseous phase (the regulating interval was 0.015 m/s). Figure 12 shows representative visualization photographs in the verification experiment. Each set of photographs in Fig. 12 was taken under the same flow conditions on the volumetric flux value of each phase. The results of experiment revealed that there appears to be little difference in the flow regimes of the diluted magnetic fluid and the distilled water. This makes sense, because the differences between the important properties of the two fluids are quite small.

The flow experiments were performed with the connected rectangular coils in a series in the same way as was done for the static experiments. Figures 13 and 14 shows the results of the flow experiment for a magnetic fluid concentration of 0.1% by volume, an input electric current of 0.25 A, a frequency of 1000 Hz, and an

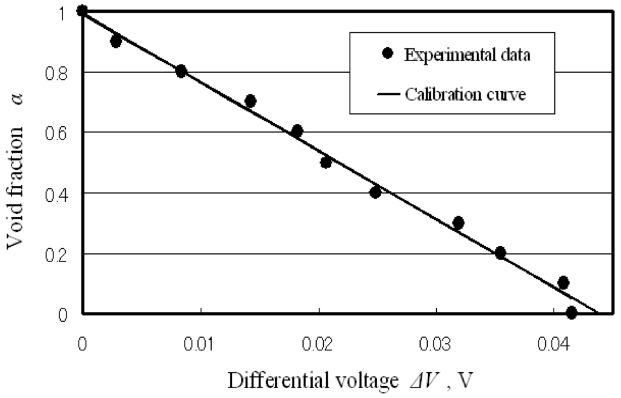

Fig. 11 Results of static experiment for various concentrations.

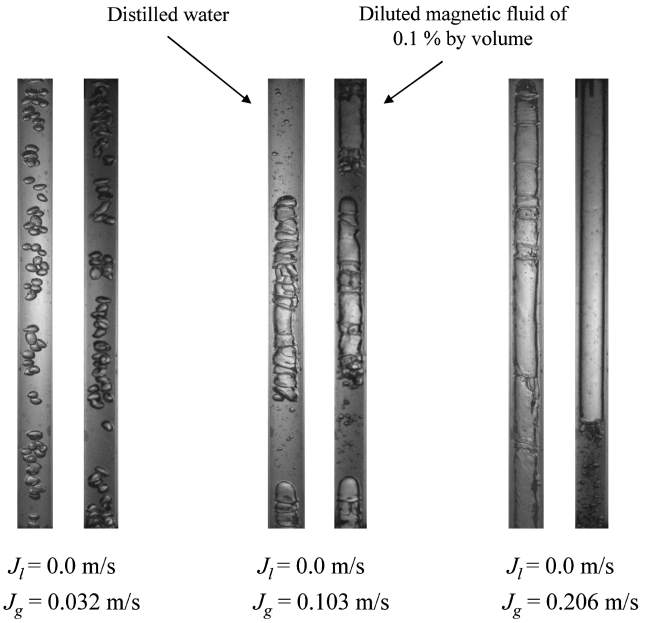

Fig. 12 Comparison of flow regime in distilled water and in diluted magnetic fluid of 0.1% by volume.

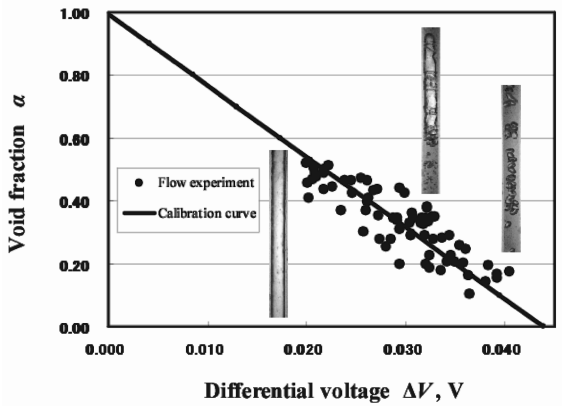

Fig. 13 Results of flow experiment [0.1 (% by volume), $j_l = 0$ (m/s)].

amplifier gain of 500. Three representative visualization photographs, taken under the same conditions on the volumetric flux value of each phase as the void fraction measurement in the flow experiment, are shown in each figure. The results in Fig. 13 are presented for the volumetric flux of the liquid phase j_l being 0 m/s and the flux of the gaseous phase j_g being 0.032–0.206 m/s. The results in Fig. 14 are presented for the volumetric flux of the liquid

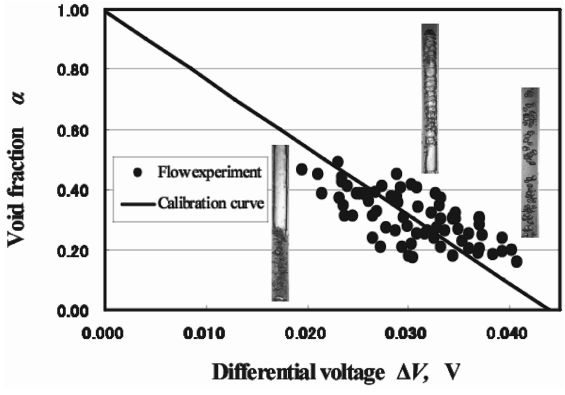

Fig. 14 Results of flow experiment [0.1 (% by volume), $j_l = 0.042$ (m/s)].

phase j_l being 0.042 m/s and the flux of the gaseous phase j_g being 0.045–0.193 m/s.

To evaluate the present method, the results of the flow experiment were compared with the calibration curve. In the experiment using $j_l = 0$ m/s, the maximum absolute error was 12.8%. It is noted that the errors (results) of the flow experiment include both error from the quick-closing valves method and error from the present measurement. The quick-closing valves method is known as a method which includes errors, and it is generally recommended to the ensemble average to minimize the error. It is found that the average of the absolute errors involved in the present experiment was 5.1%. The rms error (root mean square error) was 6.2%.

In the experiment of $j_l = 0.042$ m/s, the maximum absolute error was 16.4%. The average of the absolute errors was 7.29%. The rms error was 8.4%.

The experimental errors such as the average of absolute errors and the rms errors include the error of 0.33% associated with small temperature changes in the flow experiment. In addition, the experiments were performed over a large range of flow regimes, that is, from bubbly flow to churn-annular flow. In the present study, the water-based magnetic fluid was used for targeting applications of gas–water two-phase flow. In cases where the liquid phase is oil, the present method can be applied to applications of gas–oil two-phase flow by using oil based magnetic fluids. From the results of the flow experiments, it appears that the proposed method can be applied to the measurement of the void fraction in water–air two-phase fluids for the volumetric flux of the liquid phase j_l being 0–0.042 m/s and the flux of the gaseous phase j_g being 0–0.20 m/s.

IV. Conclusions

1) In the present experiment, the void fraction is determined by a function of differential voltage, and there is a linear relationship between the void fraction and differential voltage.

2) It has been verified theoretically that the calibration curve between the void fraction and differential voltage is linear because the error due to the bubble shape is smaller than the experimental error.

3) The results of flow experiments have indicated the practicality of the proposed method in actual gas–liquid two-phase flow.

The present study concludes that the proposed method is possibly usable as a measurement of the void fraction in air–water flow for the volumetric flux of the liquid phase j_l being 0–0.042 m/s and the flux of the gaseous phase j_g being 0–0.20 m/s. It is thought that the present method would have promise for other fluids with more conditions.

Acknowledgement

This work was supported by a Grant-In-Aid for Scientific Research (C) from the Ministry of Education, Culture, Sports, Science and Technology, Japan.

References

[1] Sakaguchi, T., Shakutsui, H., Mingawa, H., Tomiyama, A., and Takahashi, H., "Pressure Drop in Gas-Liquid-Solid Three-Phase Bubbly Flow in Vertical Pipes," *Advances in Multiphase Flow 1995*, Elsevier Science, New York, 1995, pp. 417–129.

[2] Sanaullah, K., Zaidi, S. H., and Hills, J. H., "A Study of Bubbly Flow Using Resistivity Probes in A Novel Configuration," *Chemical Engineering Journal*, Vol. 83, No. 1, 2001, pp. 45–53.

[3] Sekoguchi, H., Takeishi, M., Kano, H., Hironaga, K., and Nishimura, T., "Measurement of Velocity and Void Fraction in Gas-Liquid Two-Phase Flow with Optical Fiber," *Procceedings of the 2nd International Symposium, Application of Laser Anemometry to Fluid Mechanics*, 1984, pp. 1–5.

[4] Sekoguchi, K., Takeishi, M., Hironaga, K., and Nishimura, T., "Velocity Measurement with Electrical Double-Sensing Devices in Two-Phase Flow," *Measuring Techniques in Gas-Liquid Two-Phase Flows*, Springer, Berlin, 1984.

[5] Song, C. H., Chung, M. K., and No, H. C., "Measurements of Void Fraction by An Improved Multi-Channel Conductance Void Meter," *Nuclear Engineering and Design*, Vol. 184, No. 2, 1998, pp. 269–285.

[6] Kendoush, A. A., and Sarkis, Z. A., "Improving The Accuracy of The Capacitance Method for Void Fraction Measurement," *Experimental Thermal and Fluid Science*, Vol. 11, No. 4, 1995, pp. 311–418.

[7] Hori, K., Fujimoto, T., and Kawanishi, K., "Development of Ultra-Fast X-ray Computed Tomography Scanner System," *IEEE Transactions on Nuclear Science*, Vol. 45, No. 4, 1998, pp. 2089–2094.

[8] Mishima, K., Hibiki, T., Saito, Y., Sugimoto, J., and Moriyama, K., "Visualization Study of Molten Metal-Water Interaction by Using Neutron Radiography," *Nuclear Engineering and Design*, Vol. 189, No. 1, 1999, pp. 391–403.

[9] Prasser, H. M., Boettger, A., and Zschau, J., "A New Electrode-Mesh Tomograph For Gas-Liquid Flows," *Flow Measurement and Instrumentation*, Vol. 9, No. 2, 1998, pp. 111–119.

[10] Richter, S., Aritomi, M., Prasser, H. M., and Hampel, R., "Approach Towards Spatial Phase Reconstruction in Transient Bubbly Flow Using a Wire-Mesh Sensor," *International Journal of Heat and Mass Transfer*, Vol. 45, No. 5, 2002, pp. 1063–1075.

[11] Rosensweig, R. E., *Ferrohydrodynamics*, Cambridge Univ. Press, Cambridge, U.K., 1985, pp. 131–176.

[12] Okubo, M., Ishimoto, J., and Kamiyama, S., "Basic Study on an Energy Conversion System Using Gas-Liquid Two-Phase Flows of Magnetic Fluid," *Cavitation and Multiphase Flow*, American Society of Mechanical Engineers, Fairfield, NJ, FED-Vol. 194, 1994, pp. 105–110.

[13] Shuchi, S., Mori, T., and Yamaguchi, H., "Flow Boiling Heat Transfer of Binary Mixed Magnetic Fluid," *IEEE Transactions on Magnetics*, Vol. 38, No. 5, Sept. 2002, pp. 3234–3236.

[14] Rosensweig, R. E., *Ferrohydrodynamics*, Cambridge Univ. Press, Cambridge, U.K., 1985, pp. 74–77.

[15] Panofsky, W. K. H., and Phillips, M., *Classical Electricity and Magnetism*, Addison–Wesley Publishing Company, Reading, MA, 1955, pp. 158–163.

[16] Wangsness, R. K., *Electromagnetic Fields*, Wiley, New York, 1979, pp. 367–370.

[17] Hale, D. K., "The Physical Properties of Composite Materials," *Journal of Materials Science*, Vol. 11, No. 11, Nov. 1976, pp. 2105–2139.

[18] Landau, L. D., Lifshitz, E. M., and Pitaevskii, L. P., *Electrodynamics of Continuous Media*, 2nd ed., Pergamon Press, Oxford, England, U.K., 1984, pp. 39–44.

[19] Panofsky, W. K. H., and Phillips, M., *Classical Electricity and Magnetism*, Addison–Wesley Publishing Company, Reading, MA, 1955, pp. 144–145.

[20] Kamiyama, S., and Sato, A., "Reological Properties of Magnetic Fluids Composed of Clusters (1st, Report, Analysis of Simple Shear Flow in a Strong Magnetic Field Perpendicular to a Shearing Plane)," *JSME, Series B (Fluids and Thermal Engineering)*, Vol. B54-506, 87-0792A, Oct. 1988, pp. 2768–2777.

[21] Kaiser, R., and Miskolczy, G., "Magnetic Properties of Stable Dispersions of Subdomain Magnetic Perticles," *Journal of Applied Physics*, Vol. 41, No. 3, March 1970, pp. 1064–1072.

[22] Planck, M., *Treatise on Thermodynamics* 3rd ed., Dover Publications, New York, 1945, pp. 5–7.